Supplementary Information (SI) for Journal of Materials Chemistry A.

Modulation of intermolecular interaction in active layer Enables Highly Efficient Organic Solar Cell via introducing solid additive

Zhe Mei,[a] Rong Li,[a] Kun Li,[a] Yishi Wu,*[a] Yu Chen,[b] Hua Geng,*[a] Qing Liao,[a] Cunbin An,*[a] Hongbing Fu*[a]

[a]Beijing Key Laboratory for Optical Materials and Photonic Devices, Department of Chemistry, Capital Normal University, Beijing 100048, P. R. China. E-mail: yswu@cnu.edu.cn; hgeng@cnu.edu.cn; ancunbin@cnu.edu.cn; hbfu@cnu.edu.cn

[b]Beijing Synchrotron Radiation Laboratory, Institute of High Energy Physics, Chinese Academy of Sciences (CAS), Beijing 100049, China

Table of Contents

1. Experimental Section

1.1 Materials and Solvents

PM6, BTP-eC9 were purchased from Solarmer Materials Inc. DBB was purchased from Tokyo Chemical Industry. DIB was purchased from Sigma-Aldrich. BIB was purchased from Accela ChemBio. All organic solvents were used as received from Bei Jing TongGuang Fine Chemicals Company without further purification unless stated otherwise.

1.2 Device fabrication

Conventional OSC devices: The organic solar cells (OSCs) were fabricated with a structure of ITO/PEDOT:PSS/active layer/PDINO/Al. The ITO glasses were pretreated and sonicated with detergent water, deionized water, acetone, and isopropanol for 15 minutes. Before use, blow dry the ITO glass and then the ITO glasses were treated with PLASMA for 10 min. Afterward, the PEDOT:PSS (aqueous solution) was spin-coated on the silicon wafer at 4000 r.p.m. for 30 s. Subsequently, the ITO glasses were treated by thermal annealing for 10 min at 150 °C. The thickness of the PEDOT:PSS layer is ~ 40 nm. PM6:BTP-eC9 with the weight ratio of 1:1.2 were dissolved in chloroform at a polymer concentration of 8.5 mg mL^{-1}. The concentration of the additive is 10 mg mL^{-1}. The active-layer solutions need to be stirred at 55˚C until completely dissolved. The active-layer solutions were spin-coated onto the PEDOT:PSS layers, and then the films were treated with thermal annealing at 100˚C for 10 min. The optimal thickness of the PM6:BTP-eC9 active layer is ~ 110 nm. PDINO was dissolved in methanol at a concentration of 1 mg mL^{-1} and then spin-coated on the top of the active layers at 3000 rpm for 20 s. Finally, 110 nm Al was deposited under a high vacuum ($\sim 9\times10^{-4}$ Pa). In our laboratory, the area of OSC is 0.037 cm^2, the area of the mask is 0.0256 cm^2.

Inverted OSC devices: The pre-patterned glass/ITO was sonicated in a beaker using detergent in deionised water, deionised water, acetone, and isopropanol sequentially. After treating the ITO substrates with air plasma for 3 minutes, the sol-gel ZnO precursor solutions were spin-coated onto the ITO at 4000 rpm for 40 seconds. The substrate was then annealed at 160°C for 30 minutes. The sol-gel ZnO precursor solutions were prepared by dissolving 1.0 g of zinc acetate dihydrate and 0.28 g of monoethanolamine in 10 mL of methoxyethanol, followed by stirring overnight. Subsequently, the active layer PM6:BTP-eC9 (1:1.2) was dissolved in chloroform at a polymer concentration of 8.5 mg mL^{-1}, with the additive concentration at 10 mg mL^{-1}. The active layer solutions were stirred at 55°C until fully dissolved. These solutions were then spin-coated onto the ZnO layers, and the films were subjected to thermal annealing at 100°C for 10 minutes. The samples were transferred to a vacuum evaporation system, where 10 nm of MoO_3 and 100 nm of Ag were evaporated as the top anode using a metal aperture mask to complete device fabrication. The area of the OSC is 0.037 cm^2, while the mask area is 0.0256 cm^2.

1.3 Instruments and characterization

Ultraviolet-visible (UV-Vis) absorption spectrum was obtained from the HITACHI UH5700 spectrophotometer. The thickness values of the PEDOT:PSS and active layers were verified by a surface profilometer (Alpha-Step D-500) while the thickness of the evaporated cathodes was monitored by a quartz crystal thickness/ratio monitor (Model: STM-100/MF, Sycon). The *J–V* measurements were recorded on a source measurement unit, and the measurement was carried out under 1 sun (AM 1.5G) illumination based on a class A+AA+ solar simulator (Enlitech SS-X50). The light intensity (100 mW cm^{-2}) was calibrated by using a certified reference solar cell (Enlitech, SRC-2020 certified by NREL). The external quantum efficiency (EQE) tests were measured by using an integrated IPCE measurement system of QE-R3011 (Enli Technology Co. Ltd.).

Thermogravimetric analysis (TGA) measurements were carried out on TGA-2050 Thermogravimetry Analyze. The nanoscale morphology of blend films was observed by using Veeco Nanoscopy V atomic force microscopy (AFM) in tapping mode.

The electron mobility was measured by the space charge limited current (SCLC) method, employing a device architecture of ITO/TIPD/active layer/PDINO/Al. The hole mobility was measured by the SCLC method, employing a device architecture of ITO/PEDOT:PSS/active layer/Au. The mobilities (μ_h or μ_e) were determined by fitting the dark current to the model of a single carrier SCLC, described by the equation:

$$J = \frac{9\varepsilon_0\varepsilon_r\mu V^2}{8L^3}$$

Where J is the current, ε_0 is the permittivity of free space, ε_r is the materials relative permittivity, L is the thickness of the active layers and V is the effective voltage. The effective voltage can be obtained by subtracting the built-in voltage (V_{bi}) from the applied voltage (V_{appl}), $V=V_{appl}-V_{bi}$. The mobility can be calculated from the slope of the $J^{1/2}$-V curves.

The GIWAXS data were obtained at 1W1A Diffuse X-ray Scattering Station, Beijing Synchrotron Radiation Facility (BSRF-1W1A). CCL was calculated by Scherrer equation: d-spacing = $2\pi/q$ and CCL = $2\pi K$/FWHM, where K is shape factor (0.9 is used here), FWHM represents the full-width at half-maximum of the peak.

Transient Absorption Measurement: Time-resolved absorption spectroscopy measurements were carried out by using a HARPIA-TA spectroscopy system (HARPIA, light conversion). A fs laser with a pulse width of 190 fs and repetition rate of 100 kHz (1,030 nm, PHAROS, light conversion) was employed as the fundamental laser source of the TA system. The output of the fs laser was divided into two parts. One part was directed into an optical parametric amplifier (OPA, light conversion), and the output of OPA could be used as the pump light. The other part was used to generate probing light, that is, the white light super-continuum (WLSc). The time delay between the pump and probe was adjusted by a mechanical delay stage. All transient absorption measurements were performed at room temperature.

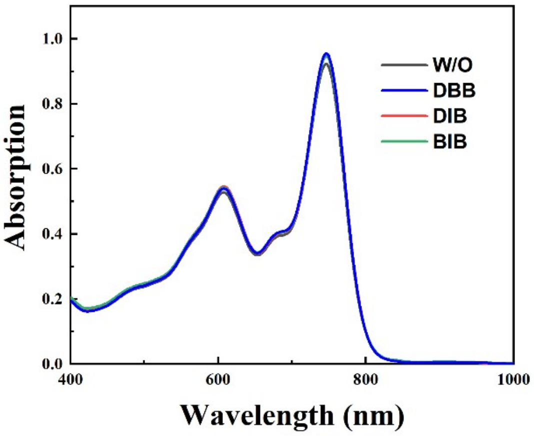

Fig. S1. Absorption spectra of PM6:BTP-eC9 (1:1.2, wt%) without and with different solid additives (10 mg mL^{-1}) in chloroform. (The concentration of PM6 is 8.87x10^{-3} mg/mL)

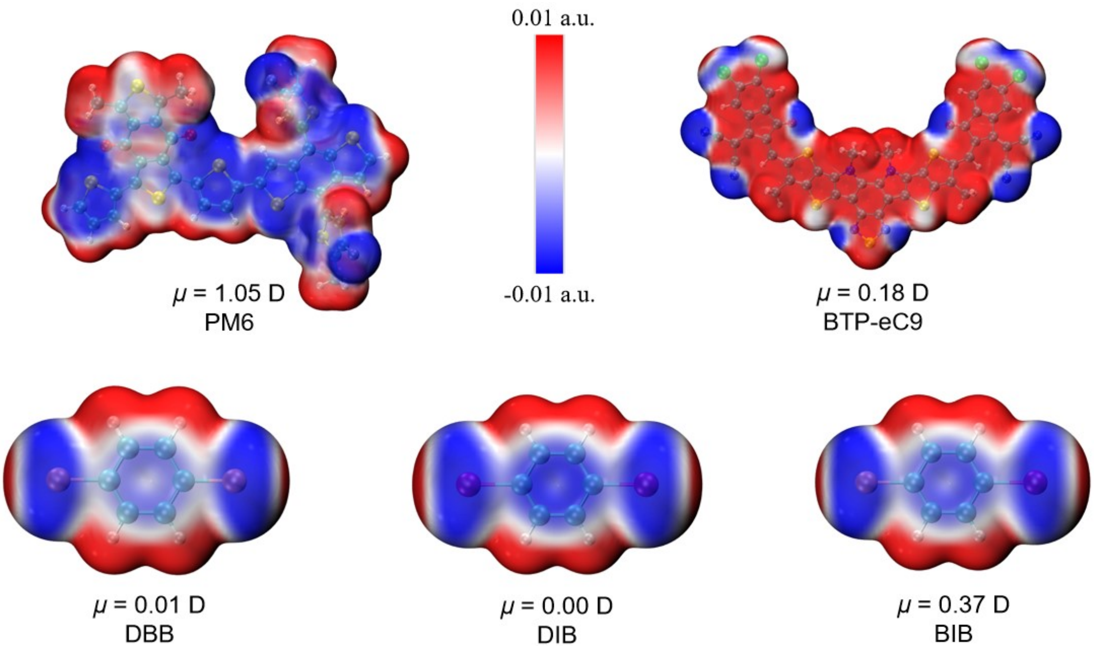

Fig. S2. The surfaces electrostatic potential distribution and dipole moments of the PM6, BTP-eC9, DBB, DIB, and BIB.

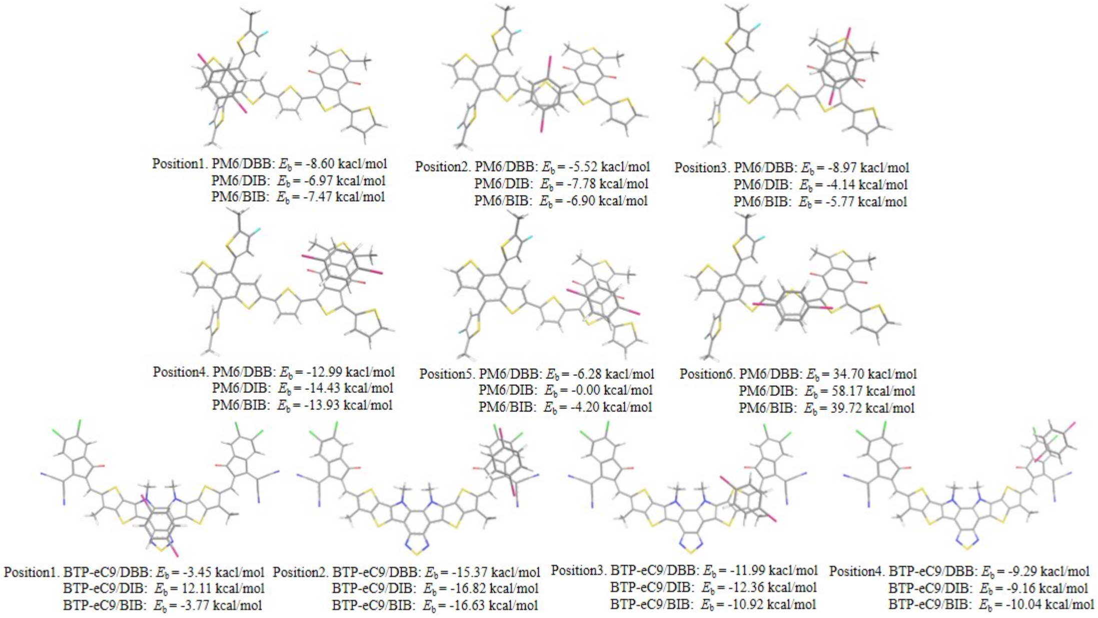
Position1. PM6/DBB: E_b = -8.60 kacl/mol
PM6/DIB: E_b = -6.97 kcal/mol
PM6/BIB: E_b = -7.47 kcal/mol

Position2. PM6/DBB: E_b = -5.52 kacl/mol
PM6/DIB: E_b = -7.78 kcal/mol
PM6/BIB: E_b = -6.90 kcal/mol

Position3. PM6/DBB: E_b = -8.97 kacl/mol
PM6/DIB: E_b = -4.14 kcal/mol
PM6/BIB: E_b = -5.77 kcal/mol

Position4. PM6/DBB: E_b = -12.99 kacl/mol
PM6/DIB: E_b = -14.43 kcal/mol
PM6/BIB: E_b = -13.93 kcal/mol

Position5. PM6/DBB: E_b = -6.28 kacl/mol
PM6/DIB: E_b = -0.00 kcal/mol
PM6/BIB: E_b = -4.20 kcal/mol

Position6. PM6/DBB: E_b = 34.70 kacl/mol
PM6/DIB: E_b = 58.17 kcal/mol
PM6/BIB: E_b = 39.72 kcal/mol

Position1. BTP-eC9/DBB: E_b = -3.45 kacl/mol
BTP-eC9/DIB: E_b = 12.11 kcal/mol
BTP-eC9/BIB: E_b = -3.77 kcal/mol

Position2. BTP-eC9/DBB: E_b = -15.37 kacl/mol
BTP-eC9/DIB: E_b = -16.82 kcal/mol
BTP-eC9/BIB: E_b = -16.63 kcal/mol

Position3. BTP-eC9/DBB: E_b = -11.99 kacl/mol
BTP-eC9/DIB: E_b = -12.36 kcal/mol
BTP-eC9/BIB: E_b = -10.92 kcal/mol

Position4. BTP-eC9/DBB: E_b = -9.29 kacl/mol
BTP-eC9/DIB: E_b = -9.16 kcal/mol
BTP-eC9/BIB: E_b = -10.04 kcal/mol

Fig. S3. The intermolecular interaction of the solid additives with PM6 and BTP-eC9 were calculated at different sites.

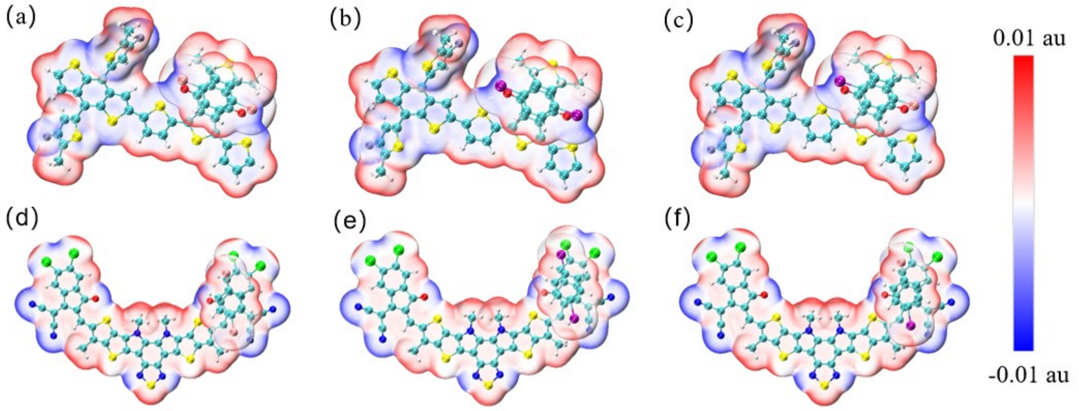

Fig. S4. The intermolecular Van der Waals surface penetration map between different additives and the active layer for (a) PM6/DBB (b) PM6/DIB (c) PM6/BIB (d) BTP-eC9/DBB (e) BTP-eC9/DIB (f) BTP-eC9/BIB.

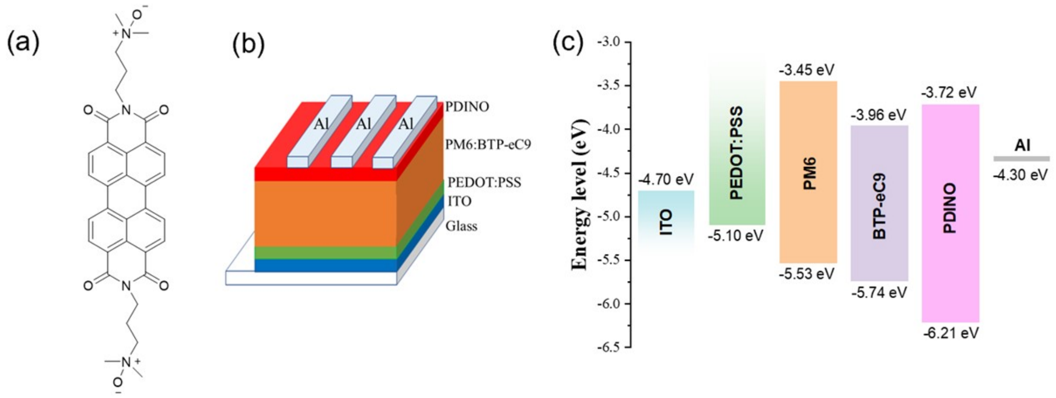

Fig. S5. (a) The chemical structure of PDINO, (b) The conventional device structure of OSC, and (c) Schematic energy level diagram of materials used in this work.

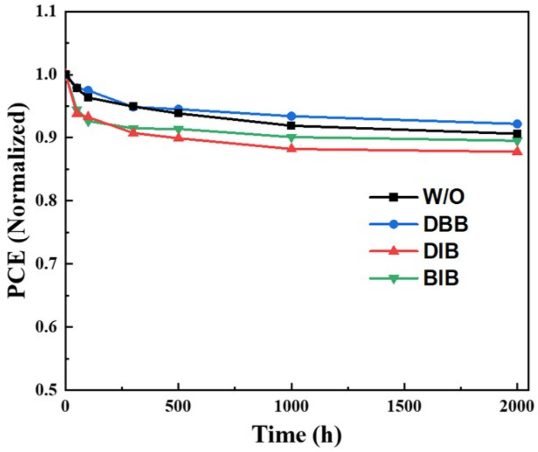

Fig. S6. Stability testing of four unencapsulated PM6:BTP-eC9-based OSCs in a glove box (H_2O: 0.01 ppm, O_2: 3.5 ppm, Temperature:25 ^{o}C).

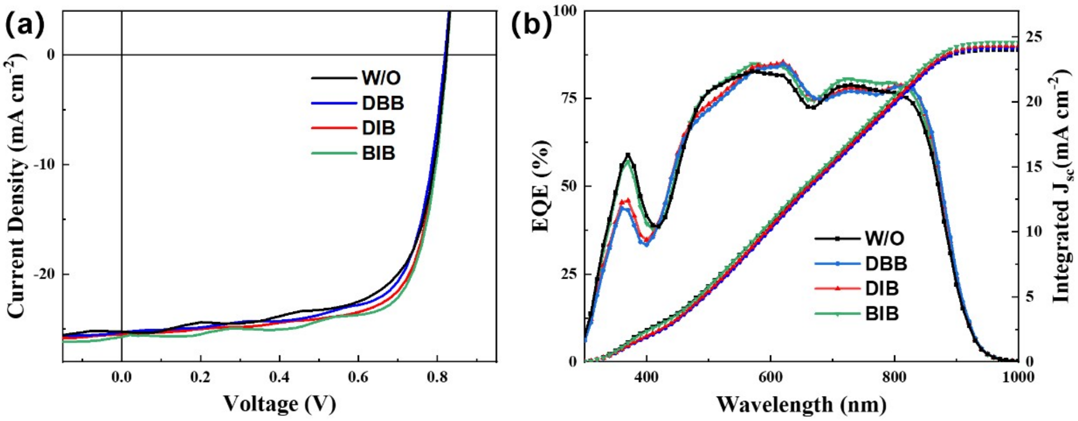

Fig. S7. (a) J–V and (b) EQE curves of the PM6:BTP-eC9-based inverted OSCs processed with different additives, under AM 1.5G illumination at 100 mW cm^{-2}.

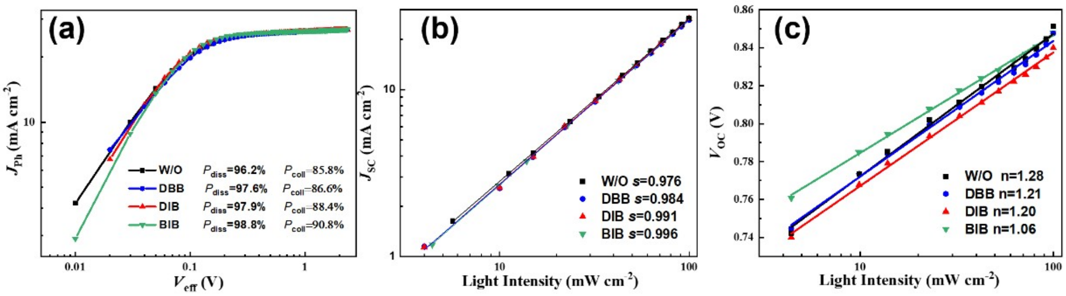

Fig. S8. (a) Plots of J_{ph} and V_{eff} of the four PM6:BTP-eC9-based OSCs; Light intensity dependence of (b) J_{SC} and (c) V_{OC} for the four PM6:BTP-eC9-based OSCs.

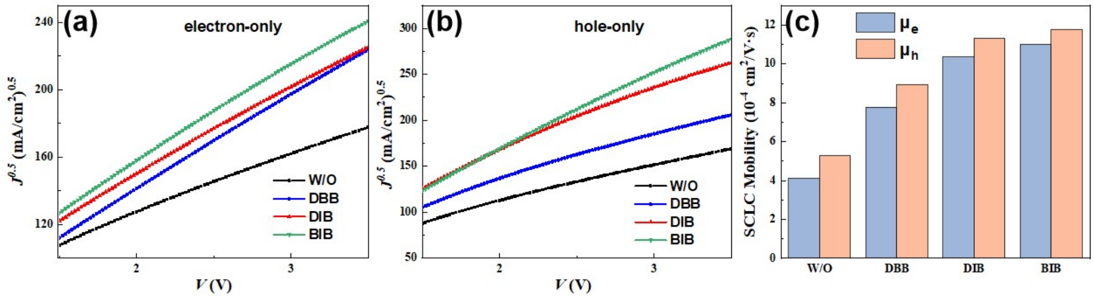

Fig. S9. SCLC method for determining electron mobilities and hole mobilities based on (a) electron-only and (b) hole-only devices using different additive-processed PM6:BTP-eC9 blend films. c) Charge mobilities histogram.

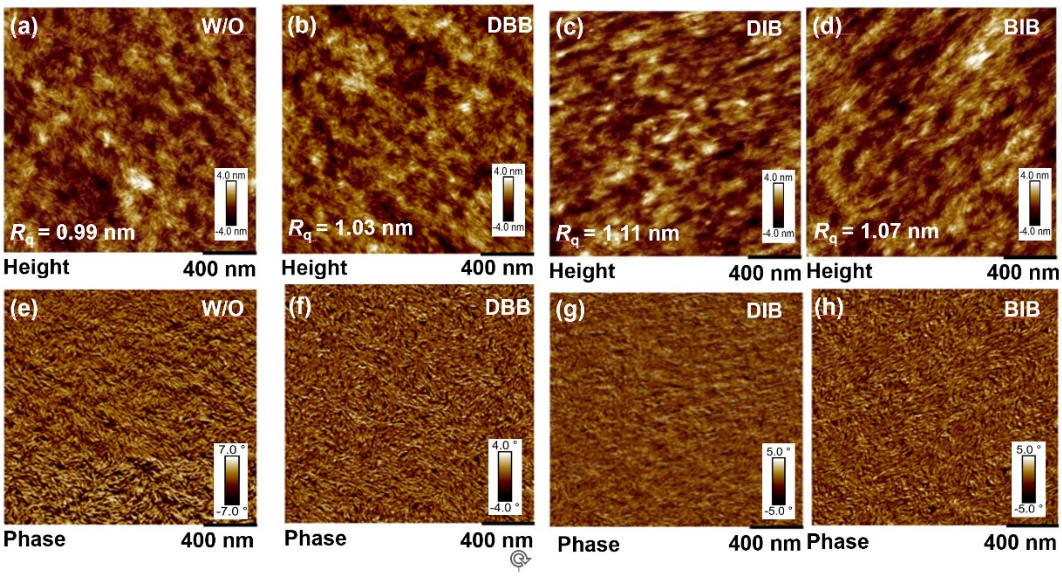

Fig. S10. AFM height images of a) W/O, b) DBB-, c) DIB-, d) BIB-processed blend films. AFM phase images of e) W/O, f) DBB-, g) DIB-, h) BIB-processed blend films.

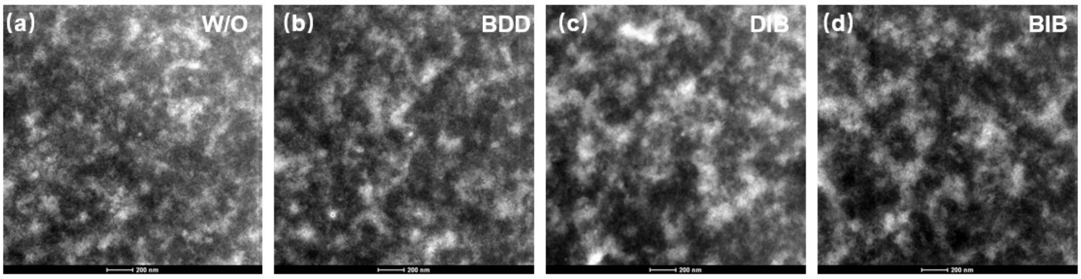

Fig. S11. TEM images of a) W/O, b) DBB-, c) DIB-, d) BIB-processed blend films.

Table S1. Quadrupole moment distribution for solid additives calculated by DFT.

SA	Q_{xx}[a)] (Debye)	Q_{YY}[b)] (Debye)	Q_{ZZ}[c)] (Debye)
DBB	-56.52	-48.51	-56.01
DIB	-67.48	-63.42	-70.91
BIB	-62.30	-55.97	-63.46

[a-c)] Quadrupole moment distribution in the x-, y-, and π–π stacking direction, respectively.

Table S2. Photovoltaic performance of the PM6:BTP-eC9-based OSCs processed by different DBB[a)] concentrations under AM 1.5G illumination at 100 mW cm^{-2}.

Concentration (mg mL^{-1})	V_{OC} (V)	FF (%)	J_{SC} (mA cm^{-2})	PCE (%)
5	0.865	73.30	26.75	16.96
10	0.862	75.83	26.22	17.14
15	0.859	73.49	26.94	17.00

[a)] The D:A ratio is 1:1.2 (weight ratio). The donor concentration is 8.5 mg/mL. The solution was heated to 55°C until total dissolution. The resulting solution was spin-coated onto PEDOT:PSS modified ITO in succession. The thickness (around 110 nm) of film was controlled the spin-coating speed at 2000-3000 rpm. Subsequently, the active layer was thermal annealed at 100°C for 10 mins.

Table S3. Photovoltaic performance of the PM6:BTP-eC9-based OSCs processed by different DIB[a] concentrations under AM 1.5G illumination at 100 mW cm^{-2}.

Concentration (mg mL^{-1})	V_{OC} (V)	FF (%)	J_{SC} (mA cm^{-2})	PCE (%)
5	0.864	74.76	26.31	17.00
10	0.862	76.77	27.58	18.25
15	0.853	76.74	26.99	17.67

[a] The D:A ratio is 1:1.2 (weight ratio). The donor concentration is 8.5 mg/mL. The solution was heated to 55°C until total dissolution. The resulting solution was spin-coated onto PEDOT:PSS modified ITO in succession. The thickness (around 110 nm) of film was controlled the spin-coating speed at 2000-3000 rpm. Subsequently, the active layer was thermal annealed at 100°C for 10 mins.

Table S4. Photovoltaic performance of the PM6: BTP-eC9-based OSCs processed by different BIB[a] concentrations under AM 1.5G illumination at 100 mW cm^{-2}.

Concentration (mg mL^{-1})	V_{OC} (V)	FF (%)	J_{SC} (mA cm^{-2})	PCE (%)
5	0.870	76.18	27.60	18.29
10	0.867	78.21	27.89	18.91
15	0.862	76.75	26.95	17.83

[a] The D:A ratio is 1:1.2 (weight ratio). The donor concentration is 8.5 mg/mL. The solution was heated to 55°C until total dissolution. The resulting solution was spin-coated onto PEDOT:PSS modified ITO in succession. The thickness (around 110 nm) of film was controlled the spin-coating speed at 2000-3000 rpm. Subsequently, the active layer was thermal annealed at 100°C for 10

mins.

Table S5. Detailed photovoltaic parameters of the optimal PM6:BTP-eC9-based inverted OSCs with different additives treatment under simulated AM 1.5G (100 mW cm^{-2}) illumination.

Additive	V_{OC} (V)	J_{SC} (mA cm^{-2})	$J_{SC, cacl.}$ (mA cm^{-2})	FF (%)	PCE (%)
W/O	0.821	25.20	24.01	67.87	14.04
DBB	0.818	25.25	24.16	70.23	14.50
DIB	0.820	25.43	24.34	71.89	15.00
BIB	0.822	25.64	24.56	73.05	15.40